Bearings-Only Maneuvering Target Motion Analysis from a Nonmaneuvering Platform

Claude Jauffret, Denis Pillon, Annie-Claude Pignol

Bearings Only Maneuvering Target Motion Analysis from a Non Maneuvering Platform

Claude JAUFFRET[*], Denis PILLON[**], Annie-Claude PIGNOL[*]

* Université Sud Toulon-Var, CNRS, IM2NP (UMR 6242) Bâtiment X, BP 132, 83957 La Garde Cedex, France, E-mail: (jauffret@univ-tln.fr, pignol@univ-tln.fr)

** Thales Underwater Systems, 525 Route des Dolines, 06903 Sophia-Antipolis, France, E-mail: (denis.pillon@fr.thalesgroup.com)

Abstract

In bearings-only target motion analysis (BOTMA), the common hypothesis is that the observer maneuvers while the source is traveling according to a constant speed and course. But there is no reason that the roles of each protagonist be not exchanged. In this paper, we consider an uncommon scenario: the trajectory of the target is composed of two legs (i.e. a target brutally changes its heading while keeping its speed) and the observer does not maneuver. We prove that the trajectory of the target is observable under non-restrictive conditions. A batch estimator is proposed and its performance is compared with the classic Cramèr-Rao lower bound (CRLB). Monte-Carlo simulations reveal the efficiency of the estimator. The robustness to a non brutal heading change is evaluated. Then an ad-hoc estimate taking the correct model into account is proposed and applied to simulated data. Again, its performance is compared to the CRLB and its robustness is evaluated when the speed of the target changes. Finally, the respective performances of the TMA made by each mobile are compared.

Keywords : Tracking, Bearings-only TMA, Maneuvering target, Observability, Cramèr-Rao Lower Bound.

I – Introduction

For the last four decades, the so-called bearings-only target motion analysis has been the subject of constant and intensive interest. If, at the very beginning, this problem was posed in an acoustic context (submarine with the use of passive sonar systems, see [2] for example), it is encountered in the electromagnetic (aircraft surveillance using ESM sensor) and optic domains (satellite using an infrared camera). The "standard" version of BOTMA assumes that the two mobiles are on the same plane and that the target has a constant course and speed (rectilinear movement) during the observation duration. As a consequence, the aim of the classical BOTMA algorithms is to estimate four parameters (two coordinates for geographical position, speed and course of a target) from a set of available bearing measurements collected by the observer.

Under those classical assumptions, it is well known ([4], [5]) that if it maintains a constant velocity vector, the own ship cannot determine the trajectory of the source. In the relative coordinate system linked to the current position of the observer, the trajectories producing the same bearings are homothetic. As a consequence, in an absolute coordinates system, the family of these trajectories is defined by three parameters ([3], [12]): the missing dimension causes the lack of observability.

This observability status is the fundamental difference between BOTMA and other TMA problems, such as the TMA based upon measurements of time difference of arrival (TDOA) or measurements of frequency difference of arrival (FDOA). In these latter cases, the source's trajectory is not observable if the source travels on a symmetry axis (for example, in TDOATMA, the source moves along the line defined by the two sensors or along their mid-perpendicular [10]). As soon as the target leaves this axis, the problem becomes observable. In short, the observability is guaranteed most of the time in TDOATMA and FDOATMA while this property is hard to obtain in BOTMA since the observer must maneuver in an efficient fashion: in BOTMA, the quality of the estimation depends highly on the observer's maneuver. Some papers propose interesting solutions to answer the difficult question: how to maneuver to get the best from the collected bearings (see [17] and [18])? On the other hand, there exist a variety of maneuvers which maintain the trajectory of the source unobservable ([4], [5]).

Any maneuver is costly for the observer which prefers to reach a point in the shortest time, i.e. by traveling along a straight line. Indeed, any zigzag will slow down the own ship. Moreover, maneuvering causes a loss of discretion with regard to another platform (which can be the target itself). For example, when maneuvering, a submarine can emit transient signals while an aircraft changes its infrared signature.

As a consequence, in BOTMA, a non-maneuvering observer which would still be able to estimate without ambiguity the trajectory of a source, would benefit from a precious advantage over many users. The way to achieve that goal is to take prior information into account. Prior information can be extra measurements, for example a given speed drawn in an admissible range (the ship's speed never exceeds 20 m/s, while the aircraft's is greater than 30 m/s) or a given course. Another way is to take other measurements into account such as the frequency line; this supposes that the source emits pure unknown and constant tones and makes a dedicated processing necessary (see [19], [25] and [30]). Frequency measurements have also been exploited for localization problems (i.e. stationary target) without the requirement of constant frequencies [31].
Bearing measurements collected by another non-maneuvering sensor make the trajectory of the source observable [20], but the price to pay is the existence of an efficient communication between the two platforms and a reliable fusion center. This link can be wireless (two submarines which communicate at a low rate) or not (for example, a towed array). In that case, except for some "pathological cases", the observability is guaranteed [5].

In this paper, we propose to consider a new piece of information when the trajectory of the source is composed of two legs ("segmented" or "piecewise rectilinear" trajectory is also the vocabulary used in the literature): the time of maneuver can be interpreted and used as an extra measurement. An assumption is required: the speed of the target must be equal to a constant.

The segmented trajectory model for the target has been widely employed in papers dealing with the problems of detecting maneuvers (see [11], [14] and [15]). Concerning the own ship maneuver, this model has been used in the past in order to propose an approximation of the CRLB [1], or to optimize the observer's maneuver [18], or to improve the optimization algorithms carried out in BOTMA (see for example [6], [7] and [8]). This model is justified since in practice, a ship or a submarine prefers to change its heading at a constant speed. Of course, a more realistic model must incorporate a part with constant turn rate between two legs: this model is widely adopted for the own ship (see [14], [16]) and for the source as well (see [13], [16] and [22]). Our proposed algorithm will be applied to some scenarios based on this model. Note that some authors have considered scenarios with a circular motion for the observer (see [21] and [22]).

In all papers dealing with bearings-only maneuvering target motion analysis (BOMTMA), the observer is supposed to maneuver before the source ([11], [14], [15]). Most of them consider recursive solutions. Here, we claim and prove that BOMTMA is feasible for a non-maneuvering own ship under non restrictive conditions. And a batch estimator reached by a numerical routine is also proposed.

The paper consists of four main sections and a conclusion:

- Section II is devoted to the presentation of BOMTMA when the source's trajectory is composed of two legs. A criterion of observability is given with its practical consequences.
- The maximum likelihood estimator is proposed in section III, the observability condition being satisfied. Some numerical details are given. Monte-Carlo simulations are also presented together with the ultimate performance given by the CRLB. Robustness to a non abrupt change is illustrated by an example.
- Section IV presents an extension of the BOMTMA to the cases of a smooth change of heading. Robustness to a small change in speed is also illustrated.
- Section V presents some tactical considerations: the respective performances of BOTMA and BOMTMA made by each mobile against the other are compared.
- The conclusion follows.

This paper is the extended version of [9].

II – BOMTMA Observability analysis and associated criterion

A. Notations and problem formulation of the BOMTMA

We consider an observer (or own ship) and a source (or target) moving on the same plane. In this section, the Cartesian coordinates will be used.

The source moves with a constant velocity vector and changes suddenly its course at time t_M to have a new heading up to the end of the scenario. More precisely, its complete motion is composed of two legs: during $[t_1 \, , \, t_M]$, the source is traveling with the velocity vector $V_{S,1}$ and during $(t_M \, , \, t_F]$ its velocity vector is $V_{S,2}$, such that $\|V_{S,1}\| = \|V_{S,2}\|$.

At any time $t \in [t_1, t_F]$, source's position vector is denoted $P_S(t)$ and the observer is positioned at $P_O(t)$. Its constant velocity vector is V_O.

As a consequence, when the chosen reference time is t_M, their respective positions at time t are described by

$$\begin{cases} P_O(t) = P_O(t_M) + (t - t_M)V_O \\ P_S(t) = P_S(t_M) + (t - t_M)V_{S,i} \end{cases} \qquad (1)$$

with $i = 1$ if $t \leq t_M$ (first leg) and $i = 2$ if $t > t_M$ (second leg). These are the basic motion equations of the BOMTMA. At this point, it is useful to introduce the following notations of the coordinates:

$$\begin{cases} P_O(t) = [x_O(t) \quad y_O(t)]^T \\ P_S(t) = [x_S(t) \quad y_S(t)]^T. \end{cases}$$

The relative velocity vector and the relative position vector of the source w.r.t. the observer are given by

$$\begin{cases} P_R(t) = P_S(t) - P_O(t) = [x_R(t) \quad y_R(t)]^T \\ \quad V_{R,i} = V_{S,i} - V_O = [\dot{x}_{R,i} \quad \dot{y}_{R,i}]^T \end{cases} \qquad (2)$$

Hence, the relative motion equation is given by

$$P_R(t) = P_R(t_M) + (t - t_M)V_{R,i}$$

with the same convention as previously : $i = 1$ if $t \leq t_M$ and $i = 2$ if $t > t_M$.

As usual in BOTMA, the noise-free bearing is then given at time *t* by

$$\theta(t) = \tan^{-1}\left[\frac{x_R(t)}{y_R(t)}\right] \quad (3)$$

A typical scenario and the associated notations are given in **Fig. 1**.

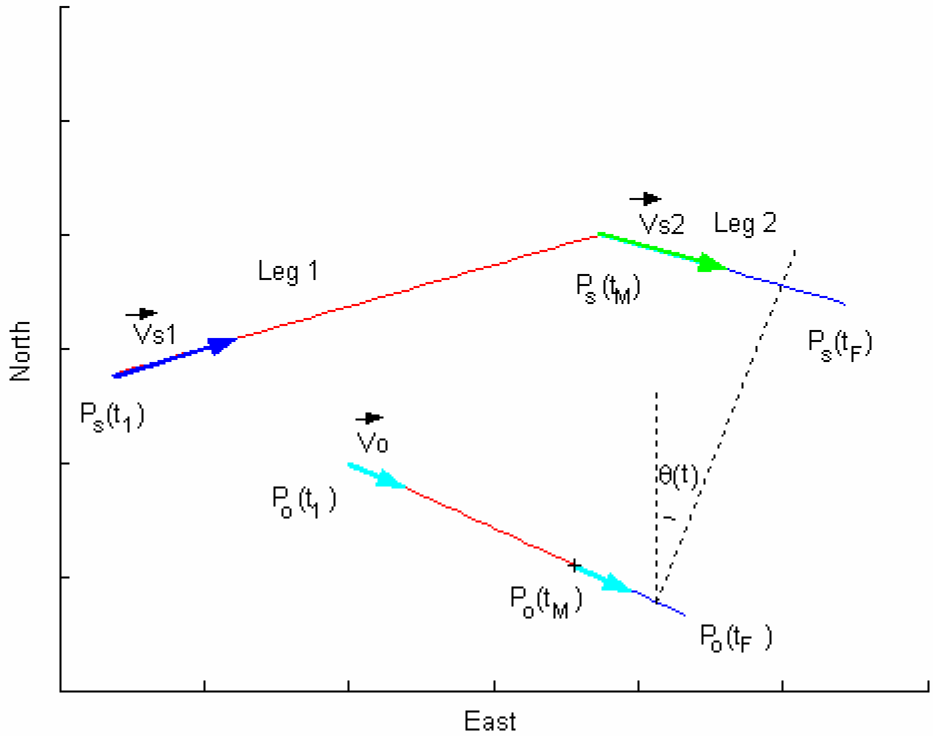

Fig. 1: Example of observer's and source's trajectories in an absolute coordinates system with $\|V_{S,1}\| = \|V_{S,2}\|$

B. Bearings-equivalent trajectories on each leg

For the sake of clarity, we will need the two following definitions:

Two sources S_1 and S_2 having their respective trajectories are said bearings-equivalent from an observer if the observer detects the two sources in the same line of sight.

Given two sources S_1 and S_2, the trajectory of S_2 is homothetic to the trajectory of S_1 w.r.t. an observer if there exists a strictly positive value λ such that

$$\begin{cases} x_{S2}(t) - x_O(t) = \lambda\,[x_{S1}(t) - x_O(t)] \\ y_{S2}(t) - y_O(t) = \lambda\,[y_{S1}(t) - y_O(t)]. \end{cases}$$

The parameter λ is called the homothetic ratio.

For one leg only, it is well known (see [3], for example) that any homothetic trajectory is bearings-equivalent to the actual one: Indeed, from (3), we get

$$\theta(t) = \tan^{-1}\left\{\frac{\lambda\,[x_S(t) - x_O(t)]}{\lambda\,[y_S(t) - y_O(t)]}\right\} = \tan^{-1}\left[\frac{\lambda\, x_R(t)}{\lambda\, y_R(t)}\right].$$

Conversely, if $\theta(t)$ is not a constant (which will be assumed subsequently), any bearings-equivalent trajectory is a homothetic trajectory. This (intuitive) statement is not trivial and we propose a proof in the appendix.

As a consequence, on each leg, the sole trajectories at a constant velocity vector and producing the same data given by (3) are defined, in the relative coordinate system whose origin is the current location of the observer, by their relative positions and velocity vectors denoted $\mathcal{P}_R(t,\lambda_i)$ and $\mathcal{V}_{R,i}(\lambda_i)$ as follows

$$\begin{cases} \mathcal{P}_R(t,\lambda_i) = \lambda_i P_R(t) \\ \mathcal{V}_{R,i}(\lambda_i) = \lambda_i V_{R,i} \end{cases} \qquad (4)$$

The homothetic ratios λ_i are strictly positive.

The corresponding trajectory is then given by (in an absolute coordinate system)

$$\begin{cases} \mathcal{V}_{S,i}(\lambda_i) = \mathcal{V}_{R,i}(\lambda_i) + V_O \\ \mathcal{P}_S(t,\lambda_i) = \mathcal{P}_R(t,\lambda_i) + P_O(t) \end{cases} \quad (5)$$

Using (4) for (5), we get

$$\begin{cases} \mathcal{V}_{S,i}(\lambda_i) = \lambda_i V_{R,i} + V_O \\ \mathcal{P}_S(t,\lambda_i) = \lambda_i P_R(t) + P_O(t) \end{cases} \quad (6)$$

Then, using (2) for (6), we obtain

$$\begin{cases} \mathcal{V}_{S,i}(\lambda_i) = \lambda_i \left[V_{S,i} - V_O\right] + V_O \\ \mathcal{P}_S(t,\lambda_i) = \lambda_i \left[P_S(t) - P_O(t)\right] + P_O(t) \end{cases} \quad (7)$$

Since the source's position at the maneuver time is unique, i.e $\mathcal{P}_S(t_M,\lambda_1) = \mathcal{P}_S(t_M,\lambda_2)$, we have the equality $\lambda_1 = \lambda_2 = \lambda$. So, (7) is simplified, as follows

$$\begin{cases} \mathcal{V}_{S,i}(\lambda) = \lambda\left[V_{S,i} - V_O\right] + V_O \\ \mathcal{P}_S(t,\lambda) = \lambda\left[P_S(t) - P_O(t)\right] + P_O(t) \end{cases} \quad (8)$$

Fig. 2 illustrates the source's trajectory and a homothetic source's trajectory in the relative coordinate system linked to the observer.

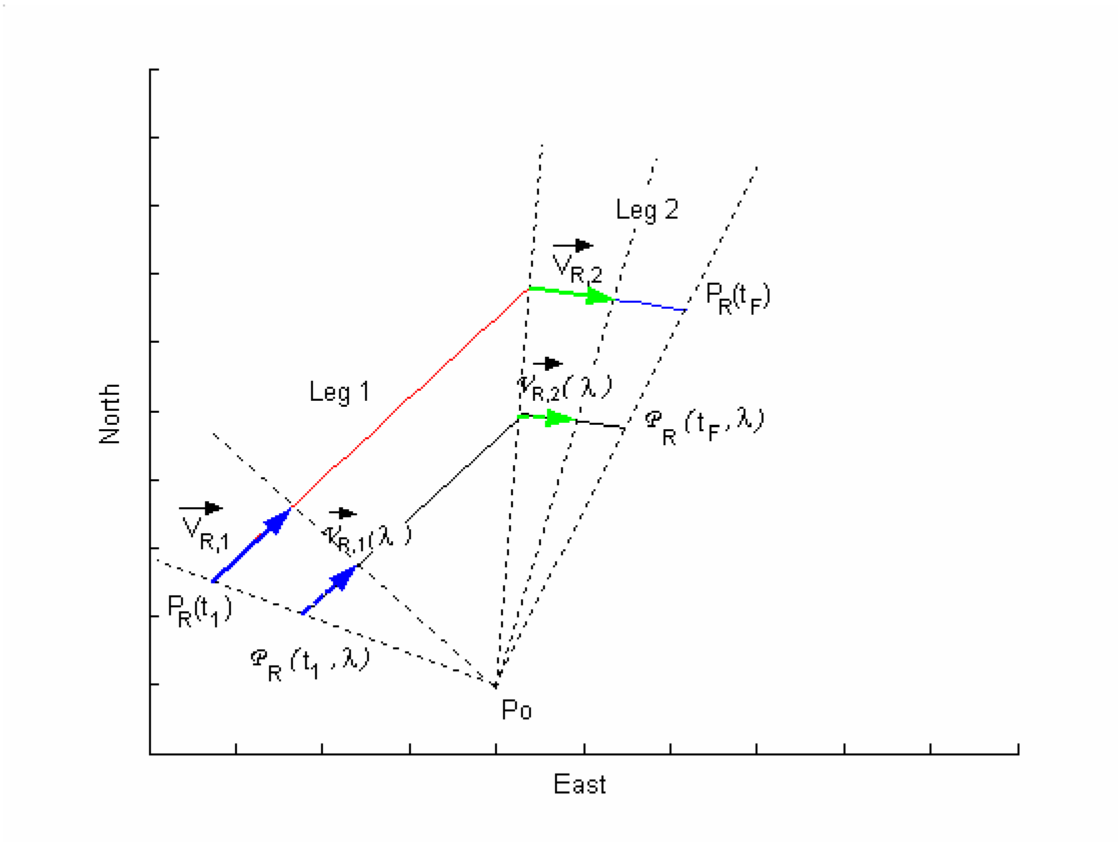

Fig. 2 : Example of source's trajectory in the relative coordinates system linked to the observer.

C. Observability analysis when t_M is known

The question of observability can be reduced to the question concerning the uniqueness of the parameter λ: if another parameter λ such as $\left\|\mathcal{V}_{S,1}(\lambda)\right\| = \left\|\mathcal{V}_{S,2}(\lambda)\right\|$ (fundamental assumption of constant speed) exists, then the trajectory is not observable, otherwise it will be.

So, let's consider the following difference:

$$\Delta v(\lambda) = \left\| \mathcal{V}_{S,1}(\lambda) \right\|^2 - \left\| \mathcal{V}_{S,2}(\lambda) \right\|^2 \qquad (9)$$

Using (8) for (9), we get

$$\Delta v(\lambda) = \left\| \lambda \left(V_{S,1} - V_O \right) + V_O \right\|^2 - \left\| \lambda \left(V_{S,2} - V_O \right) + V_O \right\|^2$$

which can be written as

$$\Delta v(\lambda) = \left\| \lambda V_{S,1} + (1-\lambda) V_O \right\|^2 - \left\| \lambda V_{S,2} + (1-\lambda) V_O \right\|^2 .$$

Using the classic formula $\left\| X + Y \right\|^2 = \left\| X \right\|^2 + \left\| Y \right\|^2 + 2X^T Y$, we get

$$\Delta v(\lambda) = 2\lambda(1-\lambda)\, V_O^T V_{S,1} - 2\lambda(1-\lambda)\, V_O^T V_{S,2} ,$$

or after factorizing

$$\Delta v(\lambda) = 2\lambda(1-\lambda)\, V_O^T \left(V_{S,1} - V_{S,2} \right).$$

We are interested in cases where $\Delta v(\lambda) = 0$. If $V_O^T \left(V_{S,1} - V_{S,2} \right) \neq 0$, then $\Delta v(\lambda) = 0$ if and only if $\lambda = 0$ or $\lambda = 1$. The solution $\lambda = 0$ must be discarded (degenerated case). The other solution ($\lambda = 1$) is acceptable and corresponds to the actual trajectory. So the condition of observability follows:

$$V_O^T \left(V_{S,1} - V_{S,2} \right) \neq 0 \qquad (10)$$

D. Practical consequences

The previous analysis implies some practical consequences:

1) The BOMTMA system is not observable if

a) $V_O = \begin{bmatrix} 0 & 0 \end{bmatrix}^T$, i.e. the observer is motionless,

b) or $V_{S,1} = V_{S,2}$, the source does not change its course, which is not our assumption,

c) or $V_O \perp \left(V_{S,1} - V_{S,2}\right)$. Note that this condition holds whatever the initial positions of the two mobiles.

2) The “special symmetric geometry” of the scenario proposed in [1] (see **Fig. 3**) satisfies the last condition $V_O \perp \left(V_{S,1} - V_{S,2}\right)$: when the role of target and own-ship are inverted, such a scenario allows one to perform an efficient BOTMA of our observer, while our observer cannot estimate the source’s trajectory!

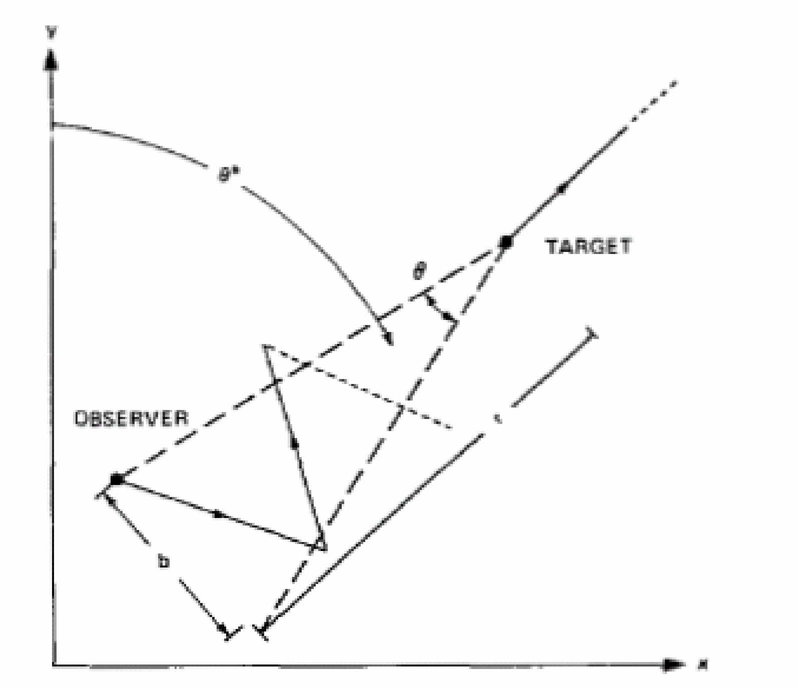

Fig. 3 : The "special symmetric geometry" (copy from [1] page 780)

3) In practice, a maneuver detection informs us about the existence of the maneuver between t_1 and t_F. Nevertheless, the two-leg trajectory of the source

can still be unobservable, see for example, the "special symmetric geometry" of the **Fig. 3**.

4) If the trajectory of the source is composed of several legs, the BOMTMA observability is guaranteed if two consecutive velocity vectors satisfy the criterion (10).

5) This conclusion is not in contradiction with previous analyses presented in [5] and [24], for example. Indeed, in those papers, the trajectory of the source is defined by a polynomial model, which is not the case here.

E. Observability analysis when t_M is unknown

We are going to prove *ab absurdo* that t_M is observable. If t_M is not observable, then there exists another instant, say t_N (arbitrary $t_M < t_N$), and a (ghost) source whose trajectory is composed of two legs : one during $[t_0,\ t_N]$ and one during $[t_N,\ t_F]$. In other words, the bearings collected during $[t_M,\ t_F]$ are generated by a non-maneuvering target (the true one) and also generated by a maneuvering target (at time t_N).

During $[t_M,\ t_N]$ then $[t_N,\ t_F]$, the two trajectories are homothetic. More precisely, the two homothetic velocity vectors of the ghost source are homothetic to the same one. In mathematical words,

- during $[t_M,\ t_F]$, the actual source has a constant relative velocity vector : $V_{R,2}$

- during $\left[t_M,\ t_N\right]$ then $\left[t_N,\ t_F\right]$, the ghost source has two constant velocity vectors, homothetic to the actual source's velocity vector : $V_{R,2}^{'}$ and $V_{R,2}^{''}$, linked to $V_{R,2}$ by

$$\begin{cases} V_{R,2}^{'} = \lambda' V_{R,2} \\ V_{R,2}^{''} = \lambda'' V_{R,2} \end{cases}$$

At t_N, the position of the ghost source is unique, so $\lambda' = \lambda'' = \lambda$. We deduce that $V_{R,2}^{'} = V_{R,2}^{''}$. Hence the ghost source does not maneuver at t_N, which is in contradiction to our assumption. Hence, t_M is observable.

Note that in this proof, the condition of observability (10) is not used. As a consequence, t_M can be estimated even though the whole trajectory is not observable.

III – Performance and robustness of the BOMTMA

We are going to construct an estimator under the observability condition (10):

$$V_O^T\left(V_{S,1} - V_{S,2}\right) \neq 0 .$$

The observer collects the measured bearings at time t_k :

$$\beta_k = \theta\left(t_k\right) + \varepsilon_k \text{ , for } k = 1,\cdots,K$$

where ε_k is the additive noise corrupting the data. As usual, the random vector $[\varepsilon_1 \ \cdots \ \varepsilon_K]^T$ is assumed to be Gaussian. It is zero-mean and its covariance matrix is equal to $diag(\sigma_k^2)$ (assumed to be known). The measurements are collected at $t_k = k\,\Delta t$. Without loss of generality, we consider also that $t_M = M\,\Delta t$. As a consequence, we will use t_M or M as well, subsequently.

A. t_M known

So far, the two-leg trajectory of the source is defined by three 2D vectors: $P_S(t_M) = [x_S(t_M) \quad y_S(t_M)]^T$, $V_{S,1}$ and $V_{S,2}$. Because $\|V_{S,1}\| = \|V_{S,2}\| = v_S$, any five component vector $Z_n = [x_S(t_n), y_S(t_n), v_S, h_{S,1}, h_{S,2}]^T$ can be helped as state vector ($h_{S,i}$ is the source's heading during leg #i). For convenience, we have chosen the state vector at time t_M denoted $Z_M = [x_S(t_M), y_S(t_M), v_S, h_{S,1}, h_{S,2}]^T$. Considering that the noise-free bearings $\theta(t_k)$ are a function of Z_M and of t_M, the noise-free measurement equation is given by

$$\theta_k(Z_M, t_M) = \tan^{-1}\left[\frac{x_S(t_M) + (t_k - t_M)v_S \sin h_{S,1} - x_O(t_k)}{y_S(t_M) + (t_k - t_M)v_S \cos h_{S,1} - y_O(t_k)}\right] = \theta_{k,1}(Z_M, t_M), \text{ if } k \le M$$

(leg 1),

$$= \tan^{-1}\left[\frac{x_S(t_M) + (t_k - t_M)v_S \sin h_{S,2} - x_O(t_k)}{y_S(t_M) + (t_k - t_M)v_S \cos h_{S,2} - y_O(t_k)}\right] = \theta_{k,2}(Z_M, t_M) \qquad \text{otherwise}$$

(leg2).

Note that with the choice of Z_n ($n \neq M$) as state vector, the mathematical expression of $\theta_k(Z_n, t_M)$ is more complicated.

1) Cramèr-Rao lower bound

The CRLB being equal to the inverse of the Fisher Information Matrix (FIM, see [28] [29]), we compute the latter as follows

$$F(Z_M) = \sum_{k=1}^{K} \frac{1}{\sigma_k^2} \nabla_{Z_M} \theta_k(Z_M, t_M) \nabla_{Z_M}^T \theta_k(Z_M, t_M)$$

where ∇_{Z_M} is the gradient operator. Then $F^{-1}(Z_M)$ is numerically evaluated.

We can easily compute $F(Z_n)$ from $F(Z_M)$ with the classic transformation

$$F(Z_n) = \Phi_{M,n}^T F(Z_M) \Phi_{M,n}$$

where $\Phi_{M,n}$ is the Jacobian of the transformation $Z_n \mapsto Z_M$, defined by

$$\begin{cases} x_S(t_M) = x_S(t_n) + (t_M - t_n) v_S \sin h_{S,i} \\ y_S(t_M) = y_S(t_n) + (t_M - t_n) v_S \cos h_{S,i} \end{cases}, \quad (11)$$

with $i = 1$ if $n < M$ and $i = 2$ otherwise, the other components of Z being unchanged:

$$\Phi_{M,n} = \begin{bmatrix} 1 & 0 & (t_M - t_n)\sin h_{S,1} & (t_M - t_n) v_S \cos h_{S,1} & 0 \\ 0 & 1 & (t_M - t_n)\cos h_{S,1} & -(t_M - t_n) v_S \sin h_{S,1} & 0 \\ 0 & 0 & 1 & 0 & 0 \\ 0 & 0 & 0 & 1 & 0 \\ 0 & 0 & 0 & 0 & 1 \end{bmatrix}, \text{ if } t_n < t_M \text{ and}$$

$$\Phi_{M,n} = \begin{bmatrix} 1 & 0 & (t_M - t_n)\sin h_{S,2} & 0 & (t_M - t_n) v_S \cos h_{S,2} \\ 0 & 1 & (t_M - t_n)\cos h_{S,2} & 0 & -(t_M - t_n) v_S \sin h_{S,2} \\ 0 & 0 & 1 & 0 & 0 \\ 0 & 0 & 0 & 1 & 0 \\ 0 & 0 & 0 & 0 & 1 \end{bmatrix}, \text{ if } t_n > t_M .$$

2) Maximum likelihood function and algorithm aspects

The maximum likelihood estimator (MLE) being equivalent to the least squared estimator if the additive noise is Gaussian and temporally uncorrelated, we have to minimize the following quadratic criterion

$$C(Z_M , t_M) = \sum_{k=1}^{K} \frac{1}{\sigma_k^2} [\beta_k - \theta_k(Z_M , t_M)]^2 .$$

We have employed the classic Newton-Raphson scheme, switching during iterations with the Levenberg-Marquardt algorithm (LMA) when necessary (for example, when the Hessian is not numerically positive definite, see [27]). The initialization point $\hat{Z}_M^0 = \left[\hat{x}_S^0(t_M), \hat{y}_S^0(t_M), \hat{v}_S^0 , \hat{h}_{S,1}^0 , \hat{h}_{S,2}^0\right]^T$ is chosen

$$\begin{cases} \hat{x}_S^0(t_M) = x_O(t_M) + \rho_M \sin\beta_M \\ \hat{y}_S^0(t_M) = y_O(t_M) + \rho_M \cos\beta_M \\ \hat{v}_S^0 = 0 \\ \hat{h}_{S,1}^0 = 0 \\ \hat{h}_{S,2}^0 = 0 \end{cases}$$

Here we have arbitrarily chosen the range (at t_M) $\rho_M = 2000m$, which is far from the true one. The routine stops as soon as the last five iterations provide five quasi identical vectors (their relative distance is less than 1%) or the maximum number of iterations is reached (this number has been fixed to 20, in our program).

The returned vector is denoted $\hat{Z}_M = \left[\hat{x}_S(t_M), \hat{y}_S(t_M), \hat{v}_S , \hat{h}_{S,1} , \hat{h}_{S,2}\right]^T$. We can readily compute, for any n, $\hat{Z}_n = \left[\hat{x}_S(t_n), \hat{y}_S(t_n), \hat{v}_S , \hat{h}_{S,1} , \hat{h}_{S,2}\right]^T$ as follows (similar to (11)

$$\begin{cases} \hat{x}_S(t_n) = \hat{x}_S(t_M) + (t_n - t_M)\hat{v}_S \sin \hat{h}_{S,2} \\ \hat{y}_S(t_n) = \hat{y}_S(t_M) + (t_n - t_M)\hat{v}_S \cos \hat{h}_{S,2} \end{cases}, \quad (12)$$

since the first two coordinates of the state vector only are different.

3) Results

For Monte-Carlo simulations, the chosen scenario is defined as follows: The observer starts from the origin; its speed is 5 m/s and its heading is 90°. Meanwhile, the source which has a speed of 4 m/s begins its trajectory at $[0\ km, 10\ km]^T$ with the initial heading of 90°. At time $t_M = 20$ min., it suddenly changes its course and its new heading is equal to 240°. The total duration of the scenario is 30 min. corresponding to a number of measurements equal to 450 (the sampling time is $\Delta t = 4s$). Hence the state vector at t_M is $Z_M = [4.8\,\text{km},\ 10\,\text{km},\ 4\,\text{m/s},\ 90°,\ 240°]^T$.

The standard deviation of the measurement noise is equal to 1°. We run 500 Monte Carlo simulations.

The statistical analysis of the 500 estimates are summarized in **Table 1** and illustrated in **Fig. 4** where the initial positions of the source (respectively the observer) is indicated by the letter “S” (respectively the letter “O”). The given statistics concern the final position of the target. The 90% confidence ellipse (corresponding to the CRLB) is plotted together with the 500 position estimates.

We note that the biases are negligible and the standard deviation of each component is close to the corresponding element of the CRLB. Obviously, the estimator performs correctly: The relative accuracy of the estimated range is

$\frac{\hat{\sigma}_\rho}{\rho} = 3.3\%$ at the final time; its relative mean-square error is equal to the same value.

Note the empirical standard deviation of the final range is defined by $\hat{\sigma}_\rho = \frac{1}{500}\sum_{i=1}^{500}\left(\hat{\rho}_i - \overline{\rho}\right)^2$, where $\hat{\rho}_i$ is the estimate of ρ at the i-th run and $\overline{\rho}$ is the empirical mean of the $\hat{\rho}_i$'s, while its relative mean-square error is defined by $\frac{1}{500}\sum_{i=1}^{500}\left(\hat{\rho}_i - \rho\right)^2$.

Table 1: performance at the final time t_K (t_M known).

Z_K	$Z_{K,True}$	$\hat{Z}_{K,average}$	Bias	σ_{CRLB}	$\hat{\sigma}$
$x_S(t_K)$	2.921km	2.897 km	0.024 km	0.153 km	0.175 km
$y_S(t_K)$	8.800 km	8.829 km	0.029 km	0.283 km	0.308 km
v_S	4 m/s	4.09 m/s	0,09 m/s	0.03 m/s	0.13 m/s
$h_{S,1}$	90°	90.57°	0.57°	12.13°	12.07°
$h_{S,2}$	240°	239.58°	0.42°	7.56°	7.53°

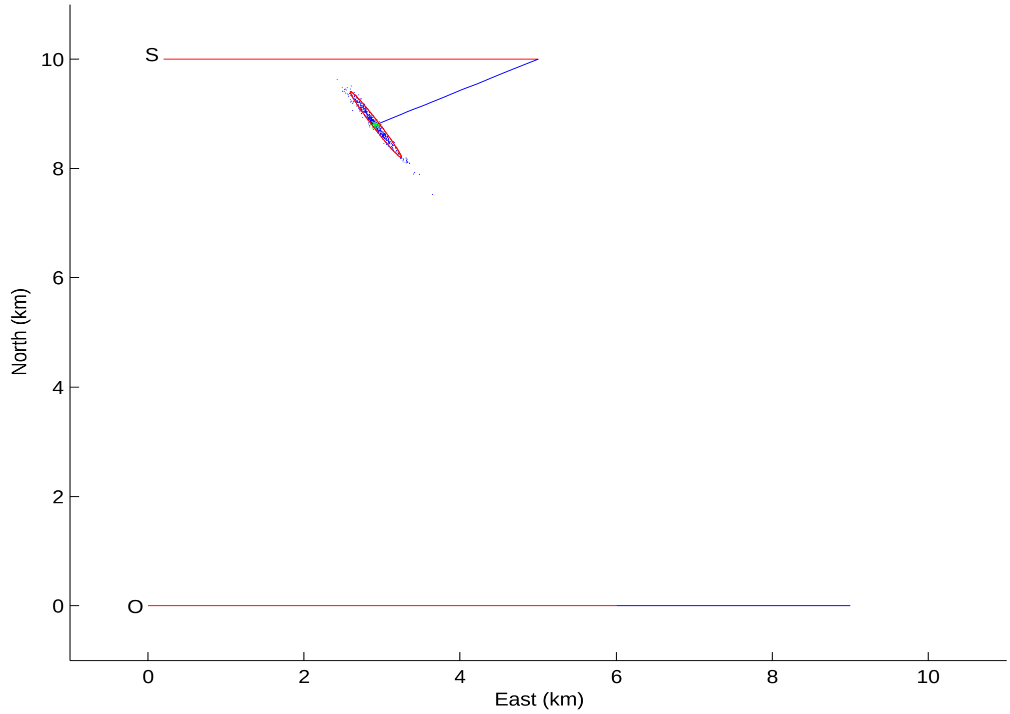

Fig. 4: Results of the Monte-Carlo runs (t_M known)

B. t_M unknown

Here, we have to estimate t_M together with Z_M which has been proven observable in section **II B**.

1) CRLB

The Fisher information matrix w.r.t. the "extended state vector" (Z_M, t_M) is not defined, since the log-likelihood function depends on $\left\lceil \frac{t_M}{\Delta t} \right\rceil$ (ceiling function of $\frac{t_M}{\Delta t}$) and is not differentiable w.r.t. t_M :

$$\operatorname{Ln} L\left(Z_M, t_M \middle| \beta_1, \cdots, \beta_K\right) = \text{Cste} \times \exp\left\{-\frac{1}{2}\sum_{k=1}^{M}\frac{1}{\sigma_k^2}\left[\beta_k - \theta_{k,1}(Z_M, t_M)\right]^2 - \frac{1}{2}\sum_{k=M+1}^{K}\frac{1}{\sigma_k^2}\left[\beta_k - \theta_{k,2}(Z_M, t_M)\right]^2\right\}$$

Consequently, the computation of the gradient of the log-likelihood function is hopeless. We have implicitly assumed that t_M is a multiple of Δt.

The Cramèr-Rao Lower Bound previously computed is here optimistic, since M is unknown and information will be shared for its estimation. However, it keeps helping as a lower bound.

2) Algorithm aspect

The following procedure is applied: for each $M \in \{3, \cdots, K-2\}$, $\hat{Z}_M$ minimizes $C(Z_M, t_M)$. Then we retain $\hat{Z}_{\hat{M}}$ (and the associated $\hat{M}$) , for which $C\left(\hat{Z}_{\hat{M}}, t_{\hat{M}}\right)$ is the least.

<u>*Remark*</u>*:* a test of maneuver detection (for example the one proposed in [11] or [23]) can be applied on the bearings, yielding a coarse estimate $\widetilde{M}$ of M. Then, a smaller search interval $\left[M_{Min}, M_{Max}\right]$ centered on $\widetilde{M}$ can be used for the algorithm.

3) Results

The Newton-Raphson (again switching with the LMA) algorithm has been initialized as previously for each M .

The statistical analysis of 500 Monte Carlo simulation runs is presented in **Table 2** and illustrated in **Fig. 5**. In **Table 2**, the results about the state vector estimator and those about the time t_M estimator are separated by three lines.

The bias and the standard deviations are a little bit greater than in the previous case (see table 1). We note that the maneuver time is correctly estimated. The relative accuracy of the estimated range is $\frac{\hat{\sigma}_\rho}{\rho} = 4\%$ at the final time while its relative mean-square error is equal to 4.07%.

Table 2: performance at the final time t_K (t_M unknown).

Z_K	$Z_{K,True}$	$\hat{Z}_{K,average}$	Bias	σ_{CRLB}	$\hat{\sigma}$
$x_S(t_K)$	2.921km	2.876km	0.045m	0.153 km	0.220 km
$y_S(t_K)$	8.800 km	8.867 km	0.067 km	0.283 km	0.370 km
v_S	4 m/s	4.11 m/s	0.11 m/s	0.03 m/s	0.19 m/s
$h_{S,1}$	90°	90.33°	0.33°	12.13°	13.18°
$h_{S,2}$	240°	240.96°	0.96°	7.56°	9.78°
t_M	1200 s	1201s	1 s	-	7 s

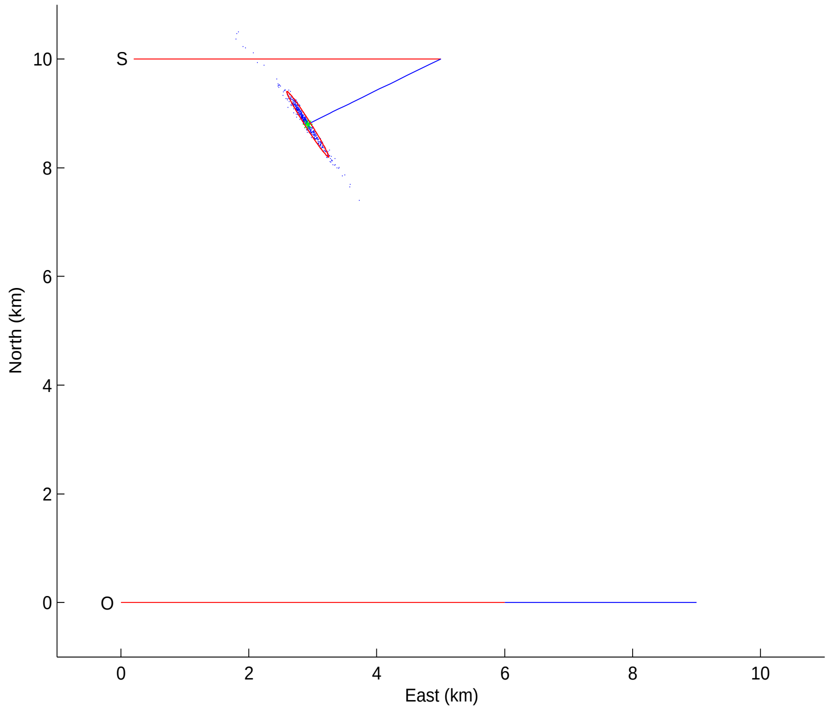

Fig. 5: Results of the Monte-Carlo runs (t_M unknown)

C. Robustness of the BOMTMA to a non abrupt change

In practice, the source does not change its heading instantaneously. This is why, it is highly important to check how robust the BOMTMA algorithm is when this assumption is violated. A new scenario has been considered: from now, the source has a constant turn rate between its two legs at constant speed.

More precisely, its trajectory is composed of

- A first leg between $[t_1,\ t_{M1})$
- Then, a arc of a circle during $[t_{M1},\ t_{M2})$
- And finally a second leg during $[t_{M2},\ t_K]$

The actual values are $t_{M1} = 1200$ s and $t_{M2} = 1360$ s, corresponding to a turn rate about 1°/s .The other parameters are unchanged.

Again, we have had recourse to 500 Monte Carlo simulations and we have used the BOMTMA algorithm of section **III B**. The results concerning this population are given in **Table 3** and illustrated in **Fig.6**.

The global performance is degraded especially concerning the estimates of the headings which are now biased. The relative accuracy of the estimated range is $\frac{\hat{\sigma}_\rho}{\rho} = 6.45\%$ at the final time and its relative mean-square error is equal to 7.17%. Note that the estimated $t_{\hat{M}}$ is almost equal to $\frac{t_{M1} + t_{M2}}{2}$.

Table 3: performance at the final time t_K (non abrupt change of heading)

Z_K	$Z_{K,True}$	$\hat{Z}_{K,average}$	Bias	$\hat{\sigma}$
$x_S(t_K)$	3.600km	3.757 km	0.157 km	0.323 km
$y_S(t_K)$	8.657km	8.375 km	0.281 km	0.575 km
v_S	4 m/s	4.14 m/s	0.14 m/s	0.19 m/s
$h_{S,1}$	90°	94.91°	4.91°	12.69°
$h_{S,2}$	240°	229.91°	10.09°	14.28°
t_{M1}	1200 s	1282 s	-	11 s
t_{M2}	1360 s			

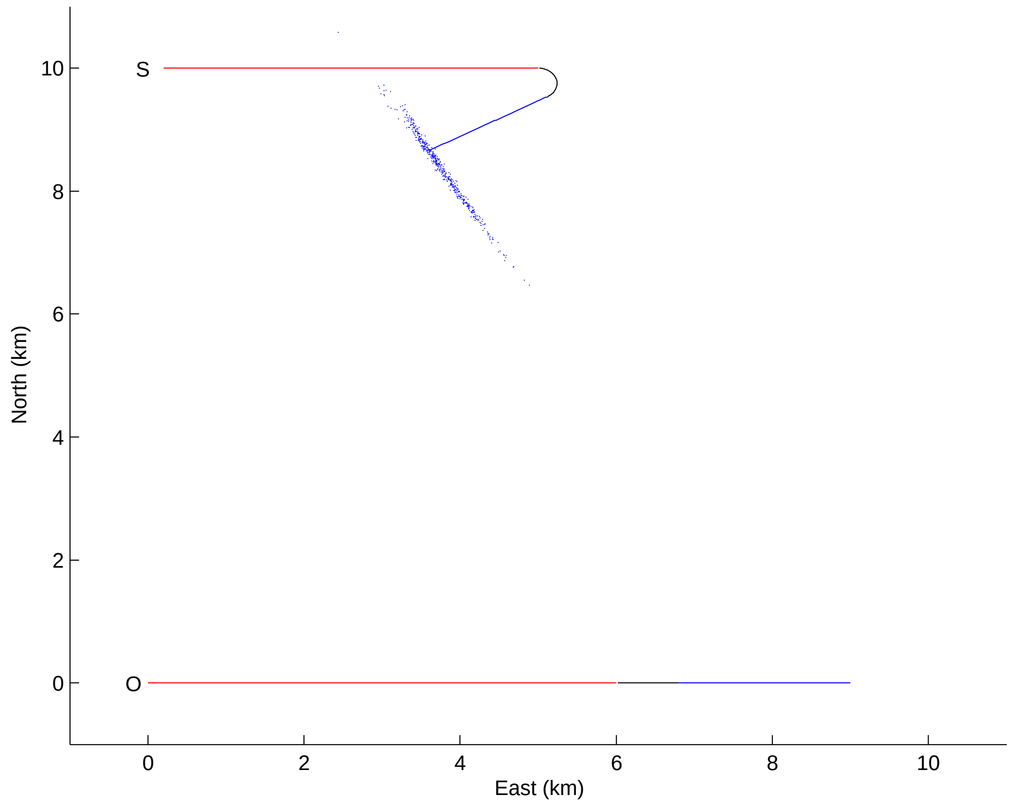

Fig. 6: Results of the Monte-Carlo runs with the leg-by-leg model

IV - Extension of the BOMTMA algorithm to a non abrupt change of heading

In the previous section (III C), we have used the leg-by-leg trajectory model. In this section, we are going to consider the correct trajectory model, taking into account the actual geometry of the source's trajectory: the source keeps a constant speed, but its trajectory is composed sequentially of a first leg at constant velocity vector, followed by a turn at constant turn rate and a second leg. The case where the beginning and the end of that turn are known will be considered; then the case where they are unknown will be studied.

A. t_{M1} *and* t_{M2} *known.*

We chose Z_K as state vector.

For convenience, the position of the source at any time t_k is given in reverse time:

- For $M_2 \le k \le K-1$ (second leg) :

$$\begin{cases} x(t_k) = x(t_K) + (k-K)\Delta t\, v \sin h_2 \\ y(t_k) = y(t_K) + (k-K)\Delta t\, v \cos h_2 \end{cases}$$

- For $M_1 \le k \le M_2 - 1$ (constant turn) :

$$\begin{cases} x(t_k) = x(t_K) + v\,\Delta t\left[(M_2-K)\sin h_2 - \sum_{i=1}^{M_2-k} \sin\left(h_1 \frac{M_2-k-i+1}{M_2-M_1+1} + h_2 \frac{k+i-M_1}{M_2-M_1+1}\right)\right] \\ y(t_k) = y(t_K) + v\,\Delta t\left[(M_2-K)\cos h_2 - \sum_{i=1}^{M_2-k} \cos\left(h_1 \frac{M_2-k-i+1}{M_2-M_1+1} + h_2 \frac{k+i-M_1}{M_2-M_1+1}\right)\right] \end{cases}$$

- For $1 \le k \le M_1 - 1$ (first leg) :

$$\begin{cases} x(t_k) = x(t_K) \\ \quad + v\,\Delta t\left[(M_2-K)\sin h_2 - \sum_{i=1}^{M_2-M_1} \sin\left(h_1 \frac{M_2-M_1-i+1}{M_2-M_1+1} + h_2 \frac{i}{M_2-M_1+1}\right) + (k-M_1)\sin h_1\right] \\ y(t_k) = y(t_K) \\ \quad + v\,\Delta t\left[(M_2-K)\cos h_2 - \sum_{i=1}^{M_2-M_1} \cos\left(h_1 \frac{M_2-M_1-i+1}{M_2-M_1+1} + h_2 \frac{i}{M_2-M_1+1}\right) + (k-M_1)\cos h_1\right] \end{cases}$$

The expression of $\theta_k(Z_K, t_{M1}, t_{M2})$ and the computation of the FIM w.r.t. Z_K follow. We did not analyze the observability; however, the FIM is numerically regular for the simulated scenario. This guarantees local observability for this scenario [26].

The quadratic criterion to minimize is

$$C(Z_K, t_{M1}, t_{M2}) = \sum_{k=1}^{K} \frac{1}{\sigma_k^2}\left[\beta_k - \theta_k(Z_K, t_{M1}, t_{M2})\right]^2 .$$

Again, 500 Monte Carlo simulations were made. Their statistical properties are given in **Table 4** and the set of estimated positions are displayed in **Fig. 7**. The relative accuracy of the estimated range is $\frac{\hat{\sigma}_\rho}{\rho} = 4.83\%$ and its relative mean-square error is equal to 5.02%.

Table 4: performance at the final time t_K (t_{M1} and t_{M2} known).

Z_K	$Z_{K,True}$	$\hat{Z}_{K,average}$	Bias	σ_{CRLB}	$\hat{\sigma}$
$x_S(t_K)$	3.600 km	3.665 km	0.065 km	0.158 km	0.231 km
$y_S(t_K)$	8.657 km	8.529 km	0.128 km	0.316km	0.437 km
v_S	4 m/s	4.06 m/s	0,06 m/s	0.026m/s	0.12 m/s
$h_{S,1}$	90°	91.78°	1.78°	8.43°	11.61°
$h_{S,2}$	240°	235.53°	4.47°	9.10°	12.27°

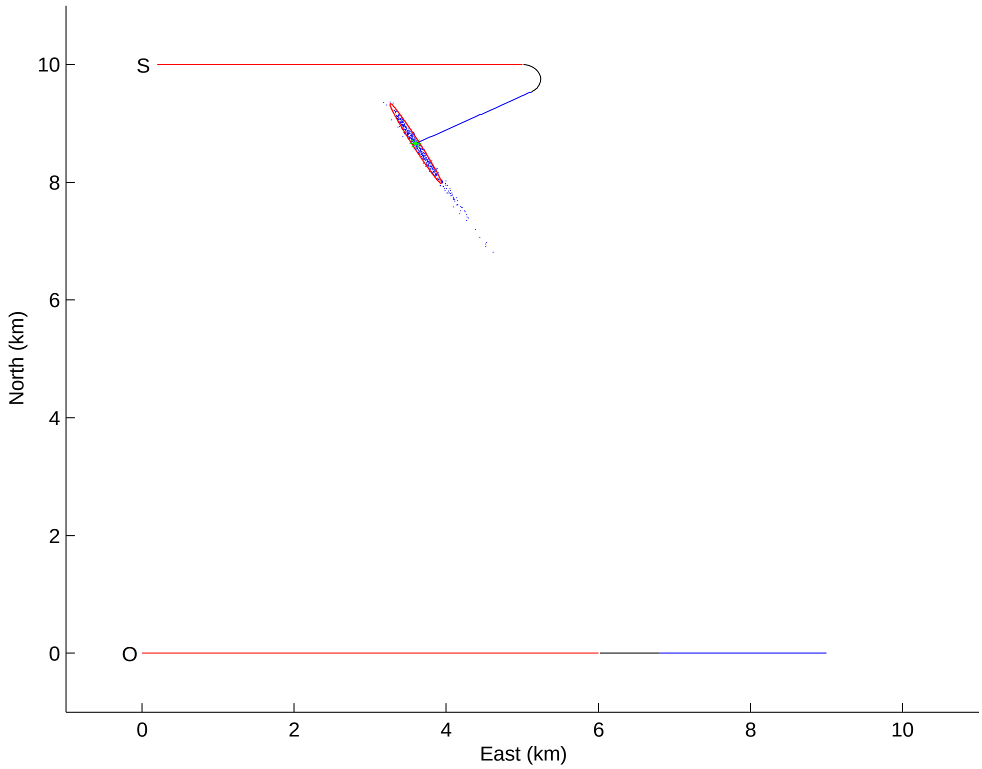

Fig. 7: Results of the Monte-Carlo runs with the correct model

B. t_{M1} and t_{M2} unknown.

The minimization of $C(Z_K, t_{M1}, t_{M2})$ w.r.t. Z_K, t_{M1} and t_{M2} follows the same scheme : for each $M1$ and $M2$ in the search set $\{3,\cdots,K-2\}$ (and $M1<M2$), we minimize $C(Z_K, t_{M1}, t_{M2})$. Again, we retain $\hat{M}1$ and $\hat{M}2$ (and the associated $\hat{Z}_K$) , for which the criterion is the least. The initialization is given by the output of the BOMTMA procedure, i.e $\hat{Z}_K$ as described in section **III B**.

The statistics of the 500 Monte Carlo simulation runs are presented in **Table 5** and illustrated in **Fig. 8**. The biases are of the same order as those presented in **Table 4**, except for the biases of the second heading which are surprisingly smaller. The standard deviations are close. The relative accuracy of the estimated range is $\frac{\hat{\sigma}_\rho}{\rho} = 5.48\%$ and its relative mean-square error is equal to 5.56%. From theses simulations, it seems that the lack of knowledge of t_{M1} and t_{M2} is not a handicap.

Table 5: performance at the final time t_K (t_{M1} and t_{M2} unknown)

Z_K	$Z_{K,True}$	$\hat{Z}_{K,average}$	Bias	σ_{CRLB}	$\hat{\sigma}$
$x_S(t_K)$	3.600 km	3.644 km	0.044 km	0.158 km	0.269 km
$y_S(t_K)$	8.657 km	8.570 km	0.087 km	0.316 km	0.492 km
v_S	4 m/s	4.105 m/s	0.105 m/s	0.026 m/s	0.177 m/s
$h_{S,1}$	90°	92.90°	2.90°	8.43°	12.54°
$h_{S,2}$	240°	237.30°	2.70°	9.10°	13.22°
t_{M1}	1200 s	1218 s	18 s	-	32 s
t_{M2}	1360 s	1345 s	15 s	-	29 s

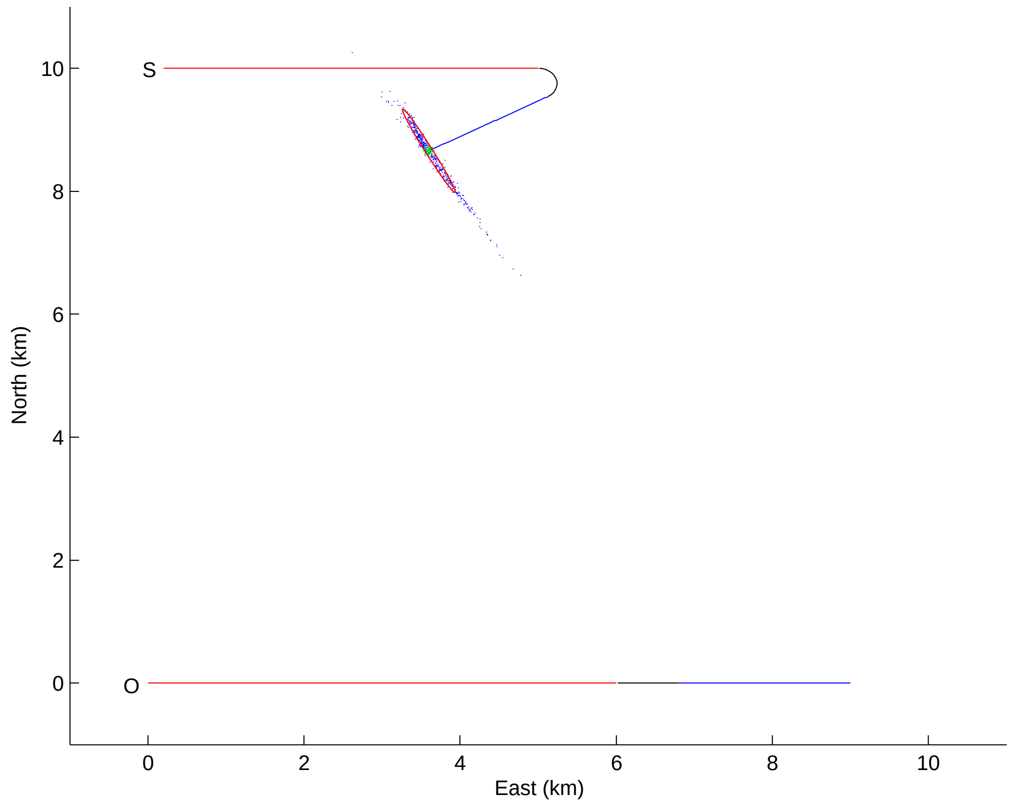

Fig. 8: Results of the Monte-Carlo runs (t_{M1} and t_{M2} unknown) with the correct model

C. Robustness of the extended BOMTMA to a small change of speed

It is interesting to check the robustness of our algorithm to a small change of speed (about 10 %). The used scenario is very similar to the previous one, except that during the second leg, the speed of the source is equal to 4.5m/s. The other parameters are unchanged. The scenario is defined by $Z'_K = \left[x_S(t_K), y_S(t_K), v_S, v_{S,2}, h_{S,1}, h_{S,2}\right]^T$. The times t_{M1} and t_{M2} are unknown.

The algorithm presented in **IV B** is then applied to 500 simulated Monte Carlo runs.

The results are summarized in **Table 6** and illustrated in **Fig. 9**. The relative accuracy of the estimated range is $\frac{\hat{\sigma}_\rho}{\rho} = 4.81\%$. Its relative mean-square error is equal to 7.47%. We observe a degradation of the performance which can be evaluated by the bias and the standard deviation of each component of $\hat{Z}_K$. Again, the estimator can be used advantageously in a real situation.

Table 6: performance at the final time t_K

(t_{M1} and t_{M2} unknown and a change of speed)

Z'_K	$Z'_{K,True}$	$\hat{Z}_{K,average}$	Bias	$\hat{\sigma}$
$x_S(t_K)$	3.404 km	3.718 km	0.314 km	0.242 km
$y_S(t_K)$	8.514km	8.023 km	0.491 km	0.428 km
v_{S1}	4 m/s	4.14 m/s	-	0.15 m/s
v_{S2}	4.5 m/s			
$h_{S,1}$	90°	92.92°	2.92°	11.79°
$h_{S,2}$	240°	236.42°	3.58°	12.00°
t_{M1}	1200 s	1223 s	23 s	30 s
t_{M2}	1360 s	1347 s	13 s	27 s

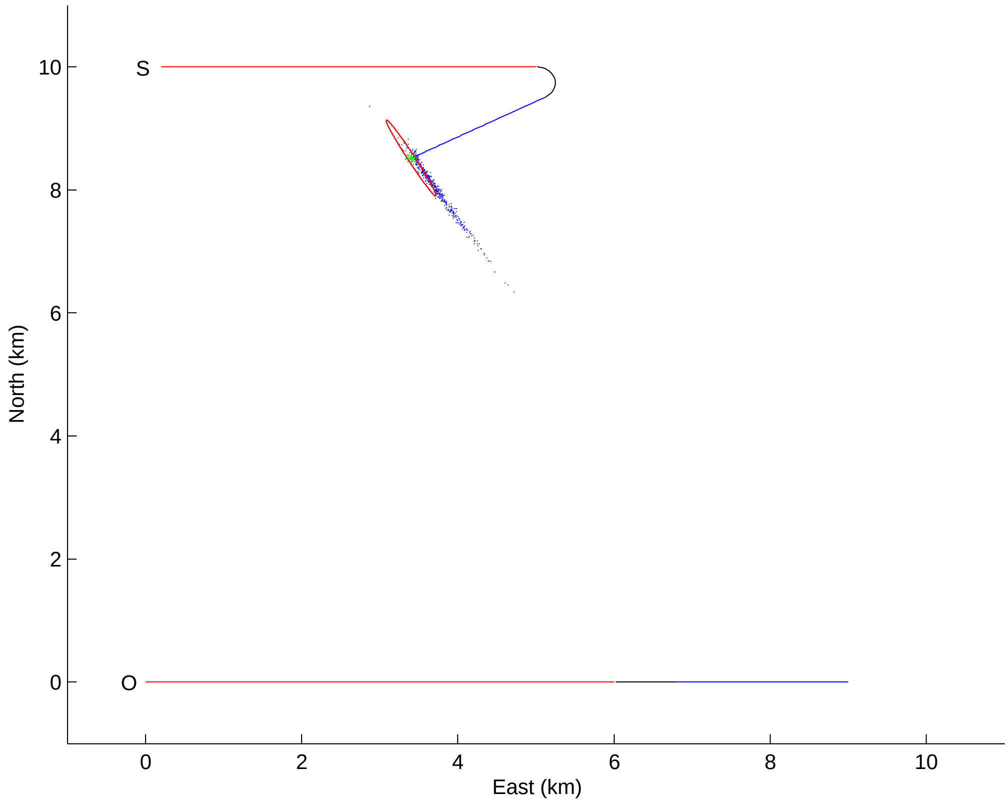

Fig. 9: Results of the Monte-Carlo runs (t_{M1} and t_{M2} unknown) with a change of speed

V - Tactical aspect

Let two mobiles be denoted by A and B. Mobile A moves at a constant velocity vector while mobile B moves on a leg at a constant velocity vector, then changes suddenly its heading but keeps its speed (in Section **II A**, A was the observer and B the source).

Each of them shall try to localize the other: mobile A by the BOMTMA and mobile B by conventional BOTMA.

We compare the accuracy of the respective estimated range, when the initial range (of the same scenario as that given in section **III A 2**) varies from 6 km to 40 km. This range accuracy is evaluated with the CRLB, the standard deviation of the measurements being equal to 1° for each platform. The values are illustrated in **Fig. 10**.

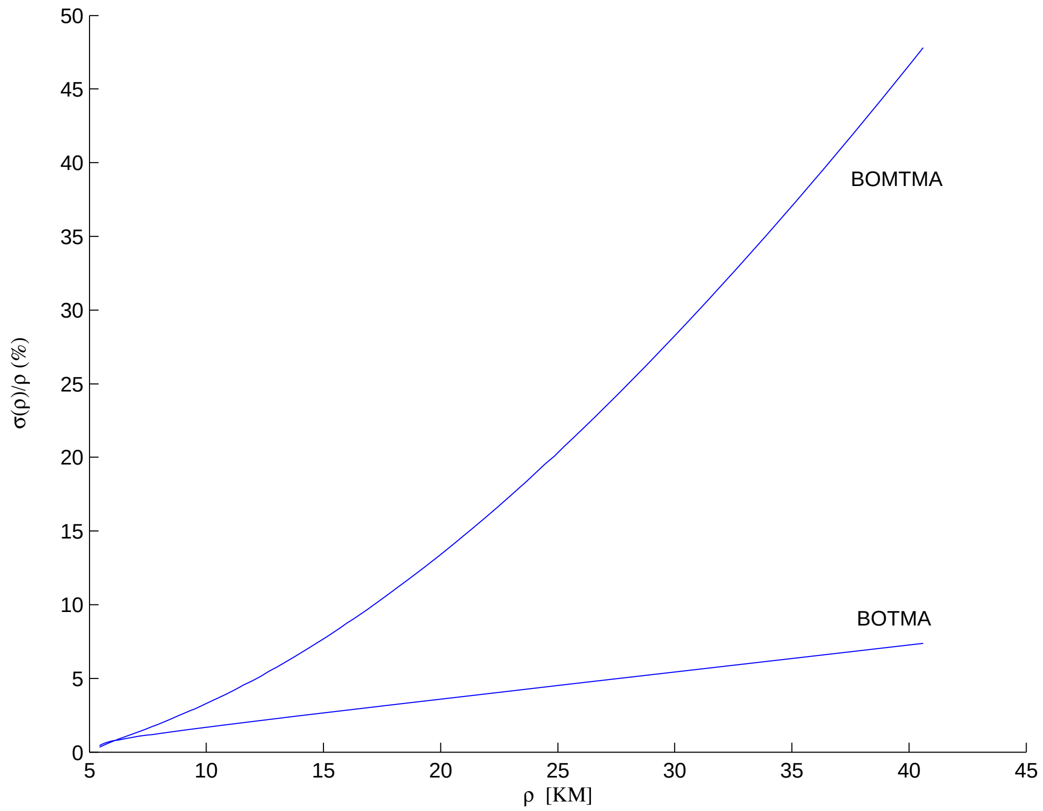

Fig. 10: relative accuracy of the range for each platform.

As expected, conventional BOTMA has advantages over BOMTMA; but mobile B must have maneuvered to realize a performing TMA, which implies a loss of discretion and other disadvantages from a tactical point of view.

We must emphasize the fact that, as noticed in paragraph **II E**, a maneuver corresponding to the "special symmetric geometry" will guarantee the supremacy of TMA of B on A, whatever the initial azimuth. An open question is then: does there exist a scenario with special geometry for which the BOMTMA overtakes the conventional BOTMA?

VI – Conclusion

Two new bearings-only tracking methods have been proposed in this paper: neither requires a maneuver of the own ship provided the source's speed does not change during the scenario and its trajectory is composed of two legs. The maneuver times need not to be known. The basic assumptions are:

- For the first method, the change of headings is instantaneous: in that case, it has been proven that the source's trajectory is observable if the bearing rate is not equal to zero and the difference of the two velocity vectors is not orthogonal to the velocity vector of the observer.

- For the second one, the two legs are separated by a turn at constant rate. The observability has not been rigorously established; in the cases treated, we have used the non-singularity of the Fisher information matrix as local observability criterion.

In both cases, a batch estimator has been proven to perform properly, in agreement with the Cramèr-Rao lower bound. **Table 7** shows that the performance is excellent since the relative mean square error on the final range (~9 km) is less than 5.6 %.

When the assumptions are violated, i.e. the speed of the target is not the same on each leg, the results are still acceptable with a relative mean square error on the final range less than 7.5 %. In the future, recursive algorithms could be applied to the same type of scenario.

For a same family of scenario, the performance analysis via the CRLB reveals the superiority of the BOTMA over the BOMTMA. This analysis must be extended to a large number of cases, before a definitive conclusion can be reached.

More generally, the observability analysis poses new tactical problems which merit a deeper analysis.

Table 7: Synthetic results about the relative range accuracy at the final time

Algorithms	Assumptions	Relative range accuracy $\frac{\sigma_\rho}{\rho}$.	Relative mean-square error on the range
BOMTMA	t_M known	3.3 %	3.3 %
	t_M unknown	4. %	4.07 %
	Non abrupt change of heading	6.45 %	7.17 %
Extended BOMTMA	t_{M1} and t_{M2} known	4.83 %	5.02 %
	t_{M1} and t_{M2} unknown	5.48 %	5.56 %
	Small change in speed	4.81 %	7.47 %

Appendix

For all the time t (except for one, at most), the bearing is given by (see (3) in **II A**)

$$\theta(t) = \tan^{-1}\left[\frac{x_R(t)}{y_R(t)}\right] \quad \forall t \in [t_1, t_F],$$

with the convenient convention that

when $y_R(t)=0$. $\theta(t)=\pi$ if $x_R(t)>0$ and $\theta(t)=-\pi$ if $x_R(t)<0$,

We start from

$$\theta(t)=\tan^{-1}\left[\frac{x_R(t^*)+(t-t^*)\dot{x}_R}{y_R(t^*)+(t-t^*)\dot{y}_R}\right] \quad \forall t\in[t_1,t_F] \quad \text{(A.1)}$$

where t^* is a reference time.

The polar coordinates of the relative position vector and of the relative velocity vector are $(\rho(t),\ \theta(t))^T$ and $(v_R,\ h_R)^T$, respectively. The correspondence between Cartesian and polar coordinates is

$$\begin{bmatrix} x_R(t) \\ y_R(t) \end{bmatrix}=\rho(t)\begin{bmatrix} \sin\theta(t) \\ \cos\theta(t) \end{bmatrix} \text{ and } \begin{bmatrix} \dot{x}_R \\ \dot{y}_R \end{bmatrix}=v_R\begin{bmatrix} \sin h_R \\ \cos h_R \end{bmatrix}. \quad \text{(A.2)}$$

Reporting (A.2) in (A.1), then, the noise-free measurement is given by

$$\begin{aligned}\theta(t)&=\tan^{-1}\left[\frac{\rho(t^*)\sin\theta(t^*)+(t-t^*)v_R\sin h_R}{\rho(t^*)\cos\theta(t^*)+(t-t^*)v_R\cos h_R}\right]\\ &=\tan^{-1}\left[\frac{\sin\theta(t^*)+(t-t^*)\dfrac{v_R}{\rho(t^*)}\sin h_R}{\cos\theta(t^*)+(t-t^*)\dfrac{v_R}{\rho(t^*)}\cos h_R}\right]\end{aligned} \quad \text{(A.3)}$$

In (A.3) the bearings are completely described by the 3-dimensional vector $Y=\left[\theta(t^*) \quad \dfrac{v_R}{\rho(t^*)} \quad h_R\right]^T=[y_1 \quad y_2 \quad y_3]^T$.

The question is then to know if the vector Y is observable.

Let $Z=(z_1 \quad z_2 \quad z_3)^T$ be another state vector, such that

$$\theta(t)=\tan^{-1}\left[\frac{\sin z_1+(t-t^*)z_2\sin z_3}{\cos z_1+(t-t^*)z_2\cos z_3}\right] \quad \forall t \qquad \text{(A.4)}$$

The question of the observability can be reformulated by

$$\tan^{-1}\left[\frac{\sin y_1+(t-t^*)y_2\sin y_3}{\cos y_1+(t-t^*)y_2\cos y_3}\right]=\tan^{-1}\left[\frac{\sin z_1+(t-t^*)z_2\sin z_3}{\cos z_1+(t-t^*)z_2\cos z_3}\right]\ \ \forall t\ \Rightarrow\ \{Z=Y\}\ ?$$

(A. 5)

If the answer is yes, the system is observable; otherwise it is not.

Two situations can be met: the first one for which $\theta(t)$ is a constant and the second one when $\theta(t)$ is not. We are going to analyze these two situations.

I - $\theta(t)$ is constant

This case is equivalent to $\dot{\theta}(t)=0\quad \forall\ t\in[t_1,t_F]$). We exploit this derivative :

$$\dot{\theta}(t)=0\quad \forall\ t\in[t_1,t_F]\ \Leftrightarrow\ \frac{d}{dt}\tan\theta(t)=0\quad \forall\ t\in[t_1,t_F]$$

Using (A.4), we obtain

$$y_2\sin y_3[\cos y_1+(t-t^*)y_2\cos y_3]-y_2\cos y_3[\sin y_1+(t-t^*)y_2\sin y_3]=0\quad \forall t$$

simplified into $\qquad y_2\sin(y_3-y_1)=0\quad \forall t$

The set of solutions is hence

$y_1=y_3$ or $y_1=\pi+y_3$ or $y_2=0$ (A6)

or equivalently

$z_1=z_3$ or $z_1=\pi+z_3$ or $z_2=0$. (A7)

Obviously, these conditions do not imply that $Z=Y$, since Y can satisfy the condition $y_1=y_3$, while Z satisfies another one, for example $z_2=0$.

In short, the 3-dimensional state vector Y is not observable when $\theta(t)$ is constant.

II - $\theta(t)$ is not constant

In this case, there does not exist an open subset of $[t_1, t_F]$ in which $\dot{\theta}(t) \neq 0$.

Note that because the bearing is not a constant, the contra poses of (A6) and (A7) stand:

$$\begin{cases} y_1 \neq y_3 \ \text{ and } \ y_1 \neq \pi + y_3 \\ \qquad \text{and } \ y_2 \neq 0 \\ \text{and } \ z_1 \neq z_3 \ \text{ and } \ z_1 \neq \pi + z_3 \\ \qquad \text{and } \ z_2 \neq 0. \end{cases}$$

The equality

$$\tan^{-1}\left[\frac{\sin y_1 + (t-t^*)y_2 \sin y_3}{\cos y_1 + (t-t^*)y_2 \cos y_3}\right] = \tan^{-1}\left[\frac{\sin z_1 + (t-t^*)z_2 \sin z_3}{\cos z_1 + (t-t^*)z_2 \cos z_3}\right] \quad \forall t \text{ implies that}$$

$$\frac{\sin y_1 + (t-t^*)y_2 \sin y_3}{\cos y_1 + (t-t^*)y_2 \cos y_3} = \frac{\sin z_1 + (t-t^*)z_2 \sin z_3}{\cos z_1 + (t-t^*)z_2 \cos z_3} \quad \forall t,$$

or equivalently that

$$\begin{aligned}&[\sin y_1 + (t-t^*)y_2 \sin y_3][\cos z_1 + (t-t^*)z_2 \cos z_3] \\ &\qquad = [\sin z_1 + (t-t^*)z_2 \sin z_3][\cos y_1 + (t-t^*)y_2 \cos y_3] \quad \forall t\end{aligned}$$

which gives us, after developing and arranging terms of the same degree

$$\begin{aligned}&\sin y_1 \cos z_1 - \sin y_1 \cos z_1 \\ &+ (t-t^*)[y_2(\sin y_3 \cos z_1 - \cos y_3 \sin z_1) + z_2(\sin y_1 \cos z_3 - \cos y_3 \sin z_1)] \\ &+ (t-t^*)^2 y_2 z_2 (\sin y_3 \cos z_3 - \cos y_3 \sin z_3) = 0 \quad \forall t\end{aligned}$$

We, hence, have to solve the system

$$\begin{cases} \sin(y_1 - z_1) = 0 & \text{(A8)} \\ y_2\sin(y_3 - z_1) + z_2\sin(y_1 - z_3) = 0 & \text{(A9)} \\ y_2 z_2 \sin(y_3 - z_3) = 0 & \text{(A10)} \end{cases}$$

From (A8), we deduce $y_1 = z_1$ (the solution $y_1 = \pi + z_1$ is not physically acceptable, since both define the line of sight). As a consequence, (A9) becomes

$$y_2\sin(y_3 - y_1) + z_2\sin(y_1 - z_3) = 0 \qquad \text{(A11)}$$

From (A10), we get $y_3 = z_3$ or $y_3 = \pi + z_3$, since neither y_2 nor z_2 are allowed to be zeroed (otherwise $\theta(t)$ would be a constant).

So we have to examine two cases:

<u>Case 1:</u> $y_3 = \pi + z_3$

Equation (A11) is then

$$y_2\sin(y_3 - y_1) - z_2\sin(y_1 - y_3) = 0$$

or

$$(y_2 + z_2)\sin(y_3 - y_1) = 0 \qquad \text{(A12)}$$

There are two possibilities only:

$$\begin{cases} \sin(y_3 - y_1) = 0 \\ \text{or } y_2 = z_2 = 0 \end{cases}$$

which is incompatible with our assumption ($\theta(t)$ is not a constant).

As a consequence, the case $y_3 = \pi + z_3$ must be discarded.

<u>Case 2:</u> $y_3 = z_3$

Equation (A11) is then $y_2\sin(y_3 - y_1) + z_2\sin(y_1 - y_3) = 0$

or equivalently $$(y_2 - z_2)\sin(y_3 - y_1) = 0 \qquad \text{(A13)}$$

The solution $\sin(y_3 - y_1) = 0$ incompatible with our assumption ($\theta(t)$ is not constant).

Hence the sole solution is $z_2 = y_2$.

All the components of Y and Z have been proved equal. As a consequence, the answer to question (A5) is yes: The 3-dimensional state vector Y is observable when $\theta(t)$ is not constant.

Summary :

If the bearing rate is not equal to zero, then the set of trajectories providing the same noise-free bearings as those originating from the source, are homothetic to the source's trajectory, both w.r.t. the observer's trajectory.

More precisely, they are defined by $\mathcal{P}_R(t,\lambda_i)$ and $\mathcal{V}_{R,i}(\lambda_i)$ as follows

$$\begin{cases} \mathcal{V}_R(\lambda) = \lambda V_R \\ \mathcal{P}_R(t,\lambda) = \lambda P_R(t) \end{cases}$$

where the homothetic ratio λ is strictly positive.

ACKNOWLEDGMENT

We are grateful to Michel Dufour for having upgraded the writing of this paper.

References

[1] Nardone, S.C., Lindgren, A.G., and Gong, K.F.

Fundamental Properties and Performance of Conventional Bearings-Only Target Motion Analysis.

IEEE Transactions on Automatic Control, **AC-29**, 9(Sept. 1984), 775-787.

[2] Kolb, R.C., Hollister, F.H.

Bearings-Only Target Motion Estimation.

In *Proceedings of the 1st Asilomar Conference on Circuits Systems,* Nov.1967.

[3] Lindgren, A.G. and Gong, K.F.

Properties of Bearings-only Motion Analysis: An interesting case study in system observability.

In *Proceedings of the 12th Asilomar Conference on Circuits Systems,* Nov. 1978.

[4] Nardone, S.C. and Aidala, V.J.

Observability Criteria for Bearings-Only Target Motion Analysis.

IEEE Transactions on Aerospace and Electronic Systems, **AES-17**, 2(Mar. 1981) 162-166.

[5] Jauffret, C., and Pillon, D.

Observability in Passive Target Motion Analysis.

IEEE Transactions on Aerospace and Electronic Systems, **AES-32**, 4(Oct. 1996) 1290-1300.

[6] Pham, D.T.

Some Quick and Efficient Methods for Bearings-Only Target Motion Analysis.

IEEE Transactions on Signal Processing, **SP- 41,** 9(Sept. 1993) 2737-2751.

[7] Nardone, S.C. and Graham, M.L.

A Closed-Form Solution to Bearings-Only Target Motion Analysis.

IEEE Journal of Oceanic Engineering, **OE-22,** 1 (Jan. 1997)168-178.

[8] Blanc-Benon, P. and Passerieux, J.M.

Fusion of Reduced-Rank TMA Estimates.

IEEE Transactions on Aerospace and Electronic Systems, **AES-36**, 3 (July 2000) 750-759

[9] Jauffret, C. Pillon, D. and Pignol, A.C.

Bearings-Only TMA Without Observer Maneuver

Proceedings of the International Conference on Information Fusion, Cologne, Germany, july 2008.

[10] Arnold, J.F., Bar-Shalom, Y., Estrada, R. and Mucci, R.A.

Target Parameter Estimation Using Measurements Acquired with a Small Number of Sensors.

IEEE Journal of Oceanic Engineering, **OE-8,** 3 (Jul. 1983) 163-171.

[11] Holst. J. and Holtsberg. A.

On Target Manoeuvres in Bearings-Only Tracking.

Proceedings of the 25th Asilomar Conference on Circuits Systems, Nov. 1991.

[12] Le Cadre, J.P. and Jauffret, C.

Discrete-time Observability and Estimability Analysis for Bearings-Only Target Motion Analysis.

IEEE Transactions on Aerospace and Electronic Systems, **AES-33**, 1 (Jan. 1997) 178-201.

[13] Kirubarajan, T., Bar-Shalom, Y. and Lerro.D

Bearings-Only Tracking of Maneuving Targets Using a Batch-Recursive Estimator.

IEEE Transactions on Aerospace and Electronic Systems, **AES-37**, 3 (Jul. 2001) 770-780.

[14] Koteswara Rao, S.
Modified Gain Extended Kalman Filter with Application to Bearings-Only Passive Manoeuvring Traget Tracking.
IEE Proceedings of Radar Sonar and Navigation., **Vol 152**, 4 (Aug. 2005) 239-244.

[15] Koteswara Rao, S.
Algorithm for Detection of Manoeuvring Targets in Bearings-Only Passive Target Tracking.
IEE Proceedings of Radar Sonar and Navigation., **Vol 146**, 3 (June 1999) 141-146.

[16] Sanjeev Arulampalam, M., Ristic, B., Gordon, N., Mansell, T.
Bearings-Only Tracking of Manoeuvring Targets Using Particle Filters.
EURASIP Journal on Applied Signal Processing, **Vol 15** (jan. 2004) 2351-2365.

[17] Passerieux, J.M., Van Cappel, D.
Optimal Observer Manoeuver for Bearings-Only Tracking.
IEEE Transactions on Aerospace and Electronic Systems, **AES-34**, 3 (Jul. 1998) 777-788.

[18] Le Cadre, J.P. and Laurent-Michel.S.
Optimizing the Receiver Maneuvers for Bearings-Only Tracking.
Automatica, **Vol 35**, (1999) 591-606.

[19] Passerieux, J.M., Pillon, D., Blanc-Benon, P. and Jauffret, C.

Target Motion Analysis with Bearings and Frequencies Measurements.

Proceedings of the 22th Asilomar Conference on Signals, Systems and Computers, Nov. 1988.

[20] Guelle, I., Pillon, D.

Inter-array Multitracks Association.

Proceedings of IEEE International Conference on Acoustics Speech and Signal Processing, (May 1989), 2744-2747.

[21] Farina, A.

Target Tracking with Bearings-Only Measurements.

Signal Processing, **Vol 78**, (1999) 61-78.

[22] Ristic, B. and Sanjeev Arulampalam, M.

Tracking a Manoeuvring Target Using Angle-Only Measurements: Algorithms and Performance.

Signal Processing, 83 (june 2003) 1223-1238

[23] Blanc-Benon, P. and Passerieux, J.M.

Trajectographie Passive en Présence d'Erreur de Modèle: Utilisation des Résidus.

Proceedings of the 12th Colloque GRETSI, Juan-les-Pins (jun. 1989)

[24] Payne, A.N.

Observability conditions for angle-only tracking

Proceedings of the 22th Asilomar Conference on Signals, Systems and Computers, Nov. 1988.

[25] Maranda, B.H. and Fawcett, J.A.

Localization of a Manoeuvring Target Using Simulated Annealing

J.Acoust. Soc. Am., **94** (3), Pt. 1, (Sept. 1993), 1376-1384.

[26] Jauffret C.

Observability and Fisher Information Matrix in Nonlinear Regression

IEEE Transactions on Aerospace and Electronic Systems, **AES-43**, pp 421-437, Apr. 2007.

[27] Dennis JE..

A User's Guide to Nonlinear Optimization Algorithms

Proceedings of IEEE, **Vol 72**, N° 12, Dec. 1984.

[28] Van Trees

Detection, Estimation, and Modulation Theory

John Wiley & Sons, 1968.

[29] Kay S.

Fundamentals of Statistical Signal Processing: Estimation Theory.

Englewood Cliffs, NJ: Prentice Hall, 1993.

[30] Becker K.

A general approach to TMA observability from angle and frequency measurements

IEEE Transactions on Aerospace and Electronic Systems, **AES-32**, pp 487-494, Jan. 1996

[31]Becker K.

Passive localization of frequency-agile radars from angle and frequency measurements

IEEE Transactions on Aerospace and Electronic Systems, **AES-35**, pp 1129-1143, Oct. 1999

Claude Jauffret born in France on March 29, 1957, received the diplôme d'Etudes Appronfondies in Applied Mathematics from Saint Charles University, Marseille, France, in 1981, the Diplôme d'Ingénieur from Ecole Nationale Supérieure d'Informatique et de Mathématiques Appliqués de Grenoble, Grenoble, France, in 1983, the title of « Docteur de l'Université » in 1993 and the « Habilitation à Diriger des Recherches » from the Université de Toulon et du Var, France.

From Nov. 1983 to Nov. 1988, he worked on passive sonar systems, more precisely on target motion analysis at GERDSM, France. After a sabbatical year at the University of Connecticut (from Nov. 1988 to Dec. 1989) during which he worked of tracking problems in cluttered environment, he developed researches in tracking, data fusion, and extraction in CERDSM. Since Sept. 1996, he has been at the Université de Toulon et du Var where he teaches statistical signal processing. His current researches are about observability, estimation in non linear systems as they appear in tracking problems.

Denis Pillon, comes from a small French mountain called "Le Jura". He received the Diplôme d'Ingénieur from Ecole Supérieure de Physique et de Chimie Industrielle (ESPCI-Paris) in 1977 and the Diplôme d'Etudes Approfondies in probability theory from the Jussieu University, Paris in 1977. From 1978 to 1979 he worked in the area of operational research at the Centre InterArmées de Recherche Opérationnelle (CIRO) agency of the Ministère de la Défense. Since 1980 he has been employed by Thomson Compagny (now Thales Compagny), France. From 1980 to 1981 he worked on sonar array processing. From 1982 to 1986, he was consultant at the GERDSM for which he worked on sea trial analysis and TMA. From 1987 to 1989, he worked on tracking and track clustering and in 1990 he was appointed group leader of signal and data processing laboratory at Thomson Sintra company, Sophia Antipolis, France. From 1992 to 1999, he was consultant at the DCN sonar laboratory. He worked on new sonar arrays and various submarine combat systems. Since 2000, he has been sonar expert at Thales Underwater Systems (Sophia-Antipolis). His current researches are about passive sonar performances estimation, submarine and torpedo array processing, and long term prospective studies for submarine warfare.

Annie-Claude Pignol born in France on November 10, 1965, received the Diplôme d'Etudes Appronfondies in Optics and Image Processing from the Université de Toulon et du Var, Toulon, France, in 1988 and the title of « Docteur de l'Université » in 1991 from the Université de Toulon et du Var, France.

Since Sept. 1994, she has been at the Université de Toulon et du Var where she teaches electronic systems. Her researches were focused signal processing applied to biomedical systems before turning them to Target Motion Analysis.